NASA / CR-1998-207664

A Two-Line Absorption Instrument for Scramjet Temperature and Water Vapor Concentration Measurement in HYPULSE

C. Y. Tsai
GASL, Inc., Ronkonkoma, New York

May 1998

The NASA STI Program Office ... in Profile

Since its founding, NASA has been dedicated to the advancement of aeronautics and space science. The NASA Scientific and Technical Information (STI) Program Office plays a key part in helping NASA maintain this important role.

The NASA STI Program Office is operated by Langley Research Center, the lead center for NASA's scientific and technical information. The NASA STI Program Office provides access to the NASA STI Database, the largest collection of aeronautical and space science STI in the world. The Program Office is also NASA's institutional mechanism for disseminating the results of its research and development activities. These results are published by NASA in the NASA STI Report Series, which includes the following report types:

- TECHNICAL PUBLICATION. Reports of completed research or a major significant phase of research that present the results of NASA programs and include extensive data or theoretical analysis. Includes compilations of significant scientific and technical data and information deemed to be of continuing reference value. NASA counter-part of peer reviewed formal professional papers, but having less stringent limitations on manuscript length and extent of graphic presentations.

- TECHNICAL MEMORANDUM. Scientific and technical findings that are preliminary or of specialized interest, e.g., quick release reports, working papers, and bibliographies that contain minimal annotation. Does not contain extensive analysis.

- CONTRACTOR REPORT. Scientific and technical findings by NASA-sponsored contractors and grantees.

- CONFERENCE PUBLICATION. Collected papers from scientific and technical conferences, symposia, seminars, or other meetings sponsored or co-sponsored by NASA.

- SPECIAL PUBLICATION. Scientific, technical, or historical information from NASA programs, projects, and missions, often concerned with subjects having substantial public interest.

- TECHNICAL TRANSLATION. English-language translations of foreign scientific and technical material pertinent to NASA's mission.

Specialized services that help round out the STI Program Office's diverse offerings include creating custom thesauri, building customized databases, organizing and publishing research results ... even providing videos.

For more information about the NASA STI Program Office, see the following:

- Access the NASA STI Program Home Page at ***http://www.sti.nasa.gov***

- E-mail your question via the Internet to help@sti.nasa.gov

- Fax your question to the NASA Access Help Desk at (301) 621-0134

- Phone the NASA Access Help Desk at (301) 621-0390

- Write to:
  NASA Access Help Desk
  NASA Center for AeroSpace Information
  7121 Standard Drive
  Hanover, MD 21076-1320

NASA / CR-1998-207664

A Two-Line Absorption Instrument for Scramjet Temperature and Water Vapor Concentration Measurement in HYPULSE

C. Y. Tsai
GASL, Inc., Ronkonkoma, New York

National Aeronautics and
Space Administration

Langley Research Center
Hampton, Virginia 23681-2199

Prepared for Langley Research Center
under Contract NAS1-19443

May 1998

Available from the following:

NASA Center for AeroSpace Information (CASI)
7121 Standard Drive
Hanover, MD 21076-1320
(301) 621-0390

National Technical Information Service (NTIS)
5285 Port Royal Road
Springfield, VA 22161-2171
(703) 487-4650

Introduction:

Scramjet combustor evaluation in ground testing relies on accurate measurement of engine thrust. When combined with the wall pressure measured, the efficiency of fuel combustion can be determined and leads to engine configuration optimization. Such thrust measurements are normally used in blowndown test facilities where the steady testing time is in the order of seconds. However, in pulse test facilities this practice is generally not available because of the short test duration. Engine performance determination in pulse facility therefore requires other direct measurements.

Temperature measurement based on 2-line water vapor absorption has become one of the most promising candidates of meeting this need. Development of TDL (Tunable Diode Laser) based water vapor temperature sensors has been undertaken in several research institutes. NASA Ames and Hanson's group at Stanford[1-6] reported the successful use of InGaAsP TDL's as water vapor sensors. Temperature of the water vapor was deduced from the ratio of direct absorption signals produced by a pair of TDL's and scanned over two water absorption lines near 1.39 μm. Recently a measurement system was packaged into a C-shape probe and installed in the CUBRC LENS shock tunnel for detection of water contamination in the facility test gas[6]. PSI, Inc. [7-9] reported the successful development of water vapor sensor using two commercially available TDL's in 1.32 μm wavelength range. The absorption signals at this wavelength was relatively low, and an IBM patented noise cancellation technique was used to enhance the S/N ratio.

A 3-beam water vapor sensor system[10] has been developed and successfully installed in NASA HYPULSE facility operated by GASL. A frequency modulation (FM) technique was used in the system to achieve higher signal/noise ratio. In the FM technique, the laser was modulated at a radio frequency (RF) of 10 MHz, while the wavelength of the laser was repeatedly scanned over about 0.14 nm by current injection at 5 kHz repetition rate. The detected RF signal was then demodulated at the modulation frequency (one-f demodulation). The FM technique thus could achieve higher detection sensitivity since the signal arose from the difference in the absorption of different sidebands as compared to the Direct Absorption (DA) methods where the signal was detected as a change against the background[11].

The system has previously been used in routine scramjet combustor testing. However, since the system only contains a single laser and only one absorption line was scanned in the test, direct temperature measurement was not available.

This technical memorandum reports the results obtained at GASL of initial development and calibration tests of a modification to the system to allow water vapor measurement over two absorption lines using a single laser for temperature determination. Successful employment of the single laser concept for the water vapor temperature and density detection could lead to the wider use of such sensors in ground test facilities and flight vehicles for engine performance measurement as it would greatly reduce the cost and space required for the sensor.

Theory:

Attenuation of the laser beam by water vapor molecules is governed by Beer's Law as:

$$I(\nu,L) = I_o \, e^{[-\alpha(\nu)\, P_a\, L]},$$

where I_o is the incident light intensity, I is the intensity after passing through the media, $\alpha(\nu)$ is the absorption coefficient, ν is the frequency, P_a is the partial pressure of water vapor, and L is the optical pathlength. The absorption coefficient can be related to the molecular line intensity, S, by

$$\alpha(\nu) = S \cdot g(\nu - \nu_o) \cdot N,$$

where $g(\nu - \nu_o)$ is the normalized lineshape function, ν_o is the frequency at line center, and N is the number density of the water vapor.

There are three lineshape profiles normally under consideration, the calculations of which and the line intensity (S) can be found in the Transmission program included in the USF Hitran-PC software package (distributed by Ontar Co., North Andover, MA). The program accesses the Hitran database[12] which provide spectroscopic data for vibrational-rotational absorption lines of 32 gases in the atmosphere over 70 –3000 K temperature range.

The Lorentzian lineshape is for pressure broadening calculations and is given as:

$$g_P(\nu - \nu_o) = (\gamma_P/\pi) / [(\nu - \nu_o)^2 + \gamma_P^2],$$

where γ_p is the pressure-broadened HWHM (half-width at half-maximum). It is related to the air-broadened parameter, g_{air} (contained in the Hitran data base with a value usually on the order of 0.05 cm^{-1}), as

$$\gamma_P = g_{air} \, (296 / T)^{0.5} \, P_t,$$

where P_t is the background pressure.

The Gaussian lineshape is for Doppler broadening and is expressed as

$$g_D(\nu - \nu_o) = (1/\gamma_D)\ (\ln 2/\pi)^{.5} \quad \exp[-\ln 2\ (\nu - \nu_o)^2 / \gamma_D^2]\ ,$$

where γ_D is the Doppler linewidth (HWHM) given by

$$\gamma_D = (\nu_o / c)[\,2\ R\ T\ \ln 2 / M\,]^{.5}$$

where c is the speed of light, R is the gas constant, T is the temperature and M is the molecular weight of the water vapor.

The Voigt profile is used for a composite of both Doppler and Pressure broadening. An approximation to the Voigt profile is given in Hitran-PC as:

$$\begin{aligned} g_V / I_{gvmax} = {} & \{[1 - (wl/wv)]\ \exp[-2.772((\nu - \nu_o)/wv)^2\,]\} \\ & + \{(wl/wv)/[\,1 + 4\ ((\nu - \nu_o)/wv)^2\,]\} \\ & + \{0.016\ [1 - (wl/wv)]\ (wl/wv)\} \\ & \{\exp[-0.4((\nu - \nu_o)/wv)^{2.25}\,] - [10/(10 + ((\nu - \nu_o)/wv)^{2.25}\,)]\,\}, \end{aligned}$$

where

$$wv = 0.5346\ wl + (\,0.2166\ wl^2 + wd^2)^{1/2}$$

$$I_{gvmax} = 1\ /\ \{\ wv * [1.065 + 0.447\ (wl/wv) + 0.058\ (wl/wv)^2\,]\ \}$$

wl, wd and wv are the FWHM linewidths of the Lorentzian, Doppler and Voigt profiles, respectively. Igvmax is the value of the Voigt profile at line center.

The above equations indicate that the temperature dependence of the water vapor transmission spectrum occurs primarily through the parameters, S, N, γ_D, and γ_p.

Hitran Prediction:

The effect of temperature on water vapor absorption was evaluated using the Hitran database and the software package. Figure 1 shows several absorption lines that are of special interest in this work. Line #1 at wavelength 1395.7 nm has previously been used in the 3-beam water vapor sensor system. A plot of the peak height versus temperature as shown in Figure 2 indicates that the line strength is low at ambient temperature, but its strength goes higher with temperature up to 1000 K and then decreases with temperature. Line #6 at wavelength 1395.5 nm was a low temperature (LT) absorption line that shows higher strength at ambient temperature and the strength continuously decreases with temperature.

The signal ratio of these two lines as illustrated in Figure 3 indicates a monotonic increase with the temperature. As compared to the ratio of the two high temperature (HT) lines used by Hanson et al, the magnitude of the HT/LT ratio is significantly higher by a factor of over five at 1500-3000 K. This greater signal ratio will lead to higher temperature sensitivity if the HT/LT sensor works. However, one drawback of using the LT line is its low line strength in the high temperature range. As shown in Figure 2, the LT absorption becomes very weak above 2500 K, possibly making detection difficult due to system noise. It was hoped that with the use of the high sensitivity FM technique the signal/noise ratio could be greatly improved and that the effect of noise interference would not become a major problem.

Experiment:

The 3-beam water vapor sensor system previously designed and installed in the HYPULSE facility was utilized in this work. Figure 4 shows schematically the current 3-beam water vapor sensor system. A single InGaAsP diode laser was used to generate infra-red emission at wavelength near 1395 nm. The laser emission was split into 3 parallel beams and placed at equal vertical distance on the side wall of the combustor module. Three detectors with optical filters and preamplifiers were placed on the opposite side of the combustor duct. The coarse tuning of the laser was made by temperature control. To obtain the line shape of the water vapor absorption feature, the laser wavelength was scanned at a rate of 5 kHz by current injection following a saw-tooth function. The current scan covered a wavelength range of about 0.16 nm. In addition to the wavelength scanning, frequency modulation at 10 MHz was used to achieve high sensitivity.

The system was removed from the scramjet test model and installed on an optical bench where a flat flame burner was used to produce water vapor at elevated temperatures. Higher current variation than that setup previously was used so that wavelength variation was sufficient to cover the whole lineshapes of both line #1 and #6 in each current scan.

The laser beams were positioned above the flat flame burner as illustrated in Figure 5. The laser and the detector were isolated from the high temperature combustion products through the use of two long steel pipes with thick wall glass windows at the ends. Both the laser and detector enclosures were continuously purged with dry nitrogen to eliminate the contribution of absorption due to ambient moisture vapor and to ensure that the laser and the detector were not subjected to heating by the combustion gas. Both windows were positioned well into the flame such that the LOS (line of sight) temperature profile within the windows was assumed to be flat.

Variation of water vapor temperature and concentration was achieved by varying the equivalence ratio and selection of fuel and oxidant. Three test series were performed using different constituents: H_2-Air, $0.4H_2$+$0.6He$-O_2, and H_2-O_2. Each test series was operated to cover the equivalence ratio range of 0.2 to 1.4. The temperature of the water vapor was estimated from the adiabatic flame temperatures corrected for the heat loss measured from the cooling water. Water concentrations were calculated for chemical equilibrium at the estimated temperature. Figures 6 and 7 show the ranges of temperature and concentration covered in the test series.

Results:

For each test point, both Direct Absorption (DA) and FM signals were recorded for 40 ms duration, i.e., a total of 200 current scans. Data from these 200 cycles were averaged and the time scale was converted to the wavelength. The DA data were then normalized to give the percentage absorption as a function wavelength. Values of absorption at the peak center for both Lines #1 and #6 were recorded. For the FM results, the peak-to-peak voltage (V_{pp}) and the peak-to-peak width (τ_{pp}) were taken. Figure 8 shows typical reduced DA and FM results.

Direct Absorption

Comparison of the DA data obtained from the H_2-Air tests (Test C) to the 3 different lineshape profiles predicted by the Hitran data base, as shown in Figure 9, indicated that the absorption of water vapor produced by H_2-Air combustion at 1 atm was best fitted by the Voigt lineshape. Consequently, the Voigt lineshape was used to infer the temperature from the DA ratio of Line #1 and #6 measured. Figure 10 indicates that the 2–line water vapor temperatures obtained agree with the estimated flame temperatures within 250 K.

With the 2-line temperatures measured, the water vapor concentrations were calculated from the absorption measured on both lines #1 and #6 using the Hitran database. Figures 11-12 show that the measured water vapor concentrations agree with results obtained from the mass flow calculation to within 10% for both lines #1 and #6. It should be noted that the uncertainty in temperature measured propagates into the concentration calculation. A greater uncertainty in temperature resulted in a higher concentration error. For the H_2-Air combustion, an underestimation of 200 K in the measured temperature would lead to a lower calculated concentration by 2% to 7% for the combustion products that have 12% to 34% water vapor, respectively.

For the H_2-He-O_2 system (Test G), a Gaussian line shape was found to better fit the data obtained (see Figure 13). Figure 14 shows that the 2-line temperatures measured agree well with the flame temperature estimated within 100 K. The water vapor concentrations reduced also agree with the mass flow calculation within 6% (see Figures 15-16).

Two test series were conducted on the H_2-O_2 combustion. In the first batch (Test D), the laser beam was position at 20 mm above the burner surface. The reduced temperatures as shown in Figure 17 indicate that greater deviations from the flame temperature were observed. Repeated tests were performed for the H_2-O_2 system. However this time (Test F) the laser beam was lowered to about 5 mm above the burner surface. The results as shown in Figure 18 show that a closer agreement with the flame temperature was achieved. However, the standard deviation for measuring temperature at this high temperature range of 2200 K to 2500 K is relatively high (about 300 K). Figures 19-20 indicate that the water vapor concentrations reduced also have greater uncertainty.

Frequency Modulation

The V_{pp} and τ_{pp} (peak to peak voltage and width) measured from the frequency modulation data were correlated to the absorption measured from the direction absorption. The correlation equations obtained then were used to convert the FM results into the degree of absorption. The same reduction procedures as used for the DA results were then performed to calculate the water vapor temperature. Figures 21-23 show the 2-line temperatures reduced for Tests C, G and F, respectively. Better agreement between the measured and the estimated flame temperatures is seen for the FM results as compared to the DA results for Test C. For Tests G and F, the FM results are comparable to the DA results. Figures 24-25 show that the deviation of the water vapor concentrations reduced from the FM signals are also decreased. The results suggest that the FM technique is a useful tool in the 2-line water vapor absorption measurement to ensure lower data errors.

Discussion and Suggestions:

Temperature and concentration measurements based on the laser line-of-sight absorption of water vapor at 1.39 mm were demonstrated. The absorption line pair selected for the 2-line temperature determination were sufficiently close together that only single laser was required. The elimination of the second laser for the 2-line temperature measurement significantly reduces the cost, size and the complexity of the water vapor sensor system. This allows installation of a large number of LOS water vapor sensors in a scramjet engine.

It is well recognized that the LOS temperature measured is an average of the temperatures along the laser beam. Values measured in conditions where temperature varies significantly along the line of sight were found to be difficult to interpret. Figure 26 can be used to illustrate this point. The data were obtained on conditions exactly the same as Test C except that the windows were positioned in a cooling nitrogen shroud surrounding the hot combustion gas core flow. The nitrogen cooling layers constituted about 5% of the total optical pathlength. It is believed that the low LOS temperatures measured were due to the presence of the low temperature water vapor layers produced upon mixing of the hot combustion gas with the cool nitrogen. The results illustrate that the lower temperature water vapor weighs much more to the LOS temperature than the high temperature vapor. The results indicate that the application of single LOS sensor is meaningful only when uniform temperature profile can be assumed or the temperature profile is known. To map a non-uniform temperature profile, a tomographic type of LOS temperature measurement is required

Reference

1. Cavolowsky, J. and Newfield, M., “Laser Absorption Flow Diagnostics for Use in Hypersonic Ground-Based and Flight Experiments,” AIAA-92-5088, 1992

2. Baer, D.S., Hanson, R.K., Newfield, M.E. and Gopaul, N.K.J.M., “Multi-Species Diode-Laser Sensor System for H_2O and O_2 Measurements,” AIAA-94-2643, 1994

3. Nagali, V., Furlong, E.R., Chou, S.I., Mihalcea, R.M., Baer, D.S. and Hanson, R.K., “Diode-Laser Sensor System for Multi-Species and Multi-Parameter Measurements in Combustion Flows,” AIAA-95-2684, 1995

4. Furlong, E.R., Baer, D.S. and Hanson, R.K., “Combustion Control Using A Multiplexed Diode-Laser Sensor,” AIAA-96-0756, 1996

5. Nagali, V., Baer, D.S. and Hanson, R.K., “Measurement of H_2O in High-Pressure Flows Using Near-IR Diode-Laser Absorption,” AIAA-96-0846, 1996

6. Wehe, S.D., Baer, D.S. and Hanson, R.K., “Tunable Diode-Laser Absorption Measurements of Temperature, Velocity, and H2O in Hypervelocity Flows,” AIAA-97-3267, 1997

7. Allen, M.G., Carleton, K.L., Davis, S.J., Kessler, W.J., Otis, C.E., Palombo, D.A. and Sonnenfroh, D.M., “Ultrasensitive Dual-Beam Absorption and Gain Spectroscopy: Applications for Near-Infrared and Visible Diode Laser Sensors,” Applied Optics, Vol. 34, No. 18, 3240-3249, 1995

8. Allen, M.G. and Kessler, W.J., “Simultaneous Water Vapor Concentration and Temperature Measurements Using 1.31-μm Diode Lasers,” AIAA Journal, Vol. 34, No. 3, 483-488, 1996

9. Miller, M.F., Rawlins, W.T and Allen, M.G., “Observations of H_2O formation in the Supersonic Combustion of H_2 by High-Enthalpy Air,” 26th Symposium (International) on Combustion/The Combustion Institute, pp. 2895-2902, 1996

10. Wang, L.G., Trucco, R.E., Sachse, G.W., Campbell R.E. and Davis, E., “Water Vapor Measurements for Combustion Diagnostics Using a 1350 nm Tunable Diode Laser,” presented at SPIE’s OE/LASE’94, 22-29 January, 1994

11. Wang, L.G., Riris, H., Carlisle, C.B. and Gallagher, T.F., “Comparison of approaches to modulation spectroscopy with GaAlAs semiconductor lasers: application to water vapor,” Applied Optics, Vol. 27, No. 10, 2071-2077, 1988

12. Rothman, L., Gamache, R., Tipping, R., Rinsland, C., Simth, M., Benner, D., Malathy Devi, V., Flaud, J.M., Camy-Peyret, C., Perrin, A., Goldman, A., Massie, S., Brown, L. and Toth, R., “The HITRAN Molecular Database: Editions of 1991 and 1992,” J. Quant. Spectrosc. Radiat. Transfer, Vol. 48, 469-507, 1992

Figure 1. Water Vapor Absorption at 1395-1396 nm
(HITRAN, l=10 mm, Pt=1 atm, %H2O=50, Lorentzian lineshape)

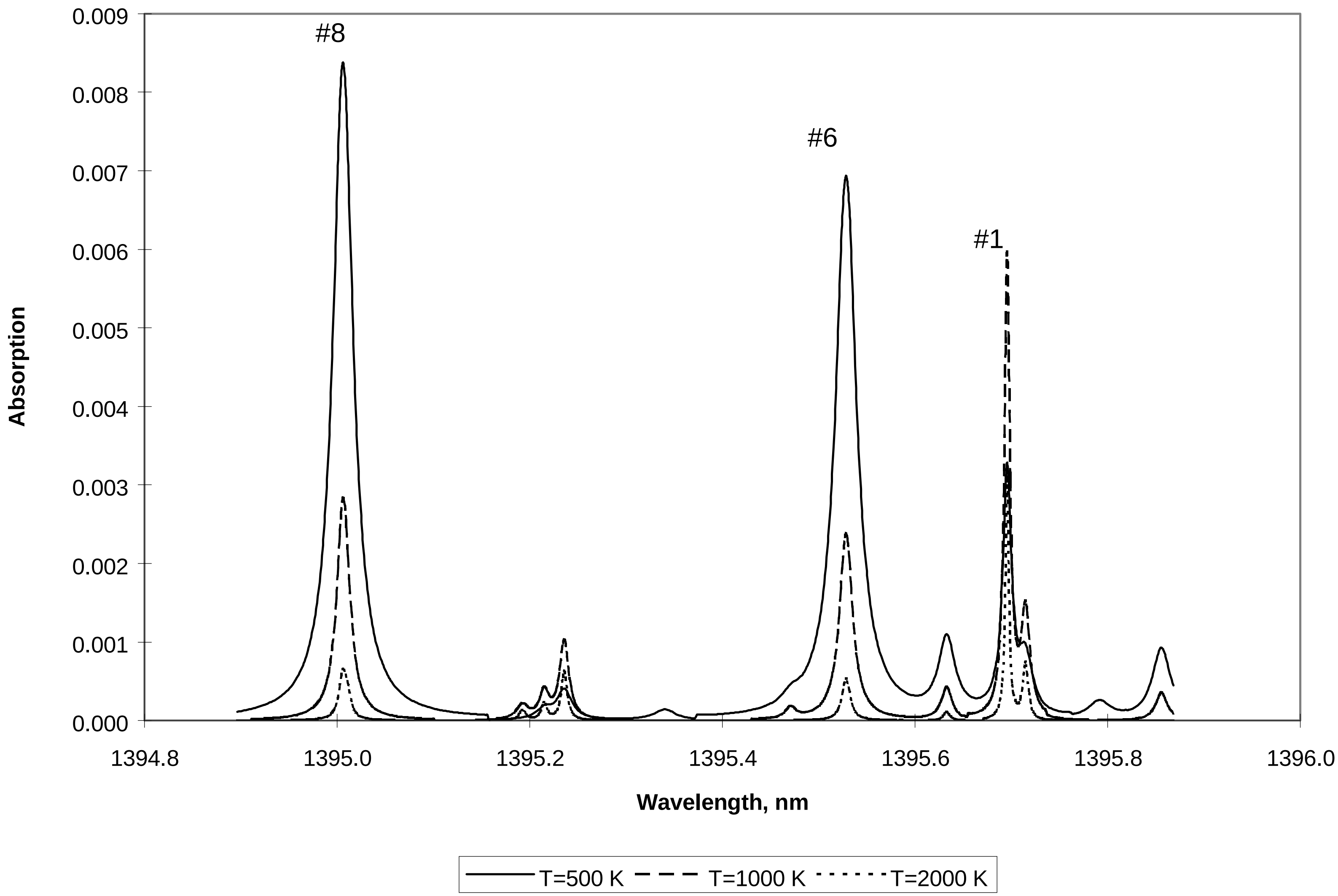

Figure 2. Effect of Temperature on Water Vapor Absorption at 1395.5 and 1395.7 nm
(HITRAN, l=10 mm, Pt=1 atm, %H2O=50, Lorentzian lineshape)

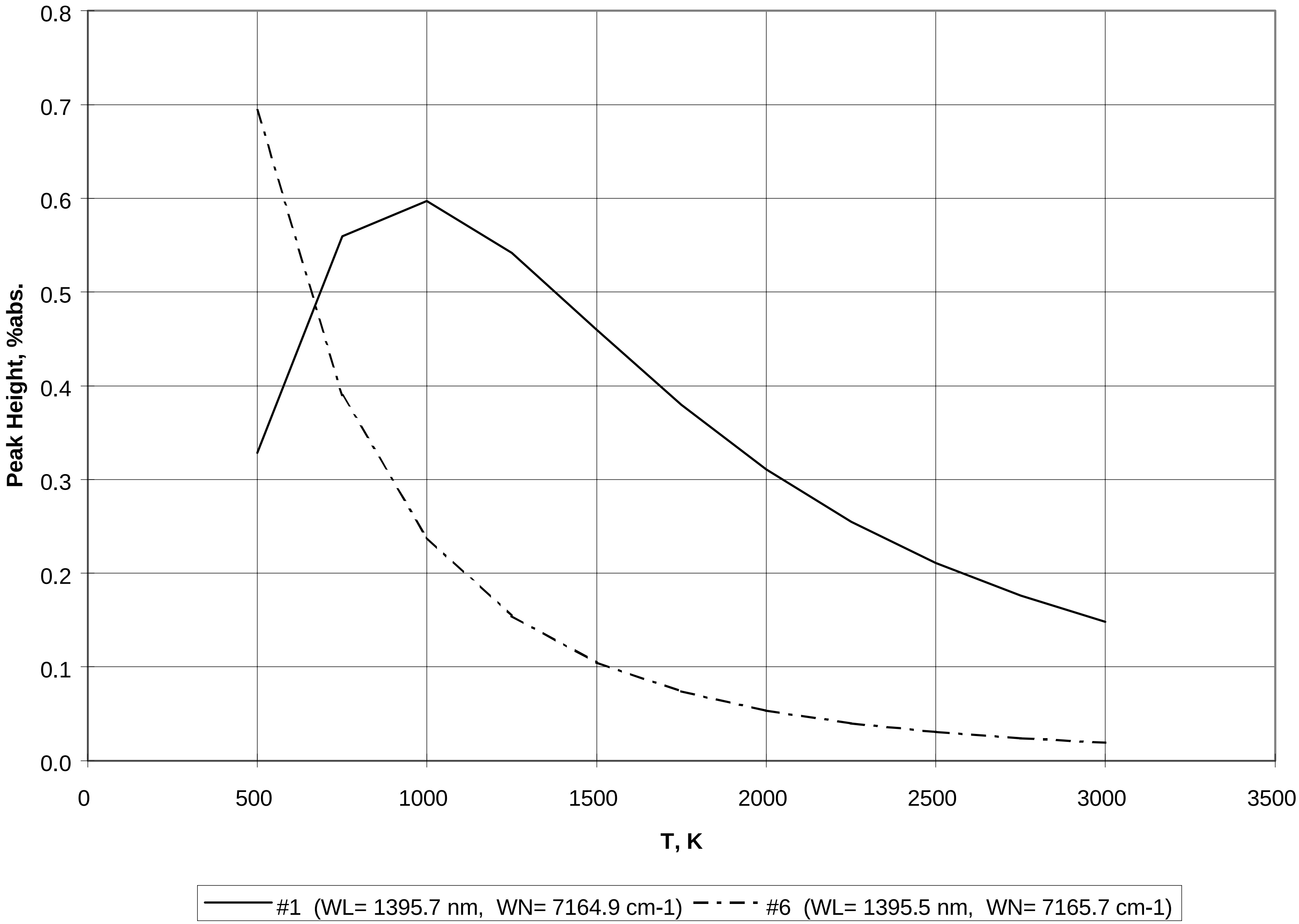

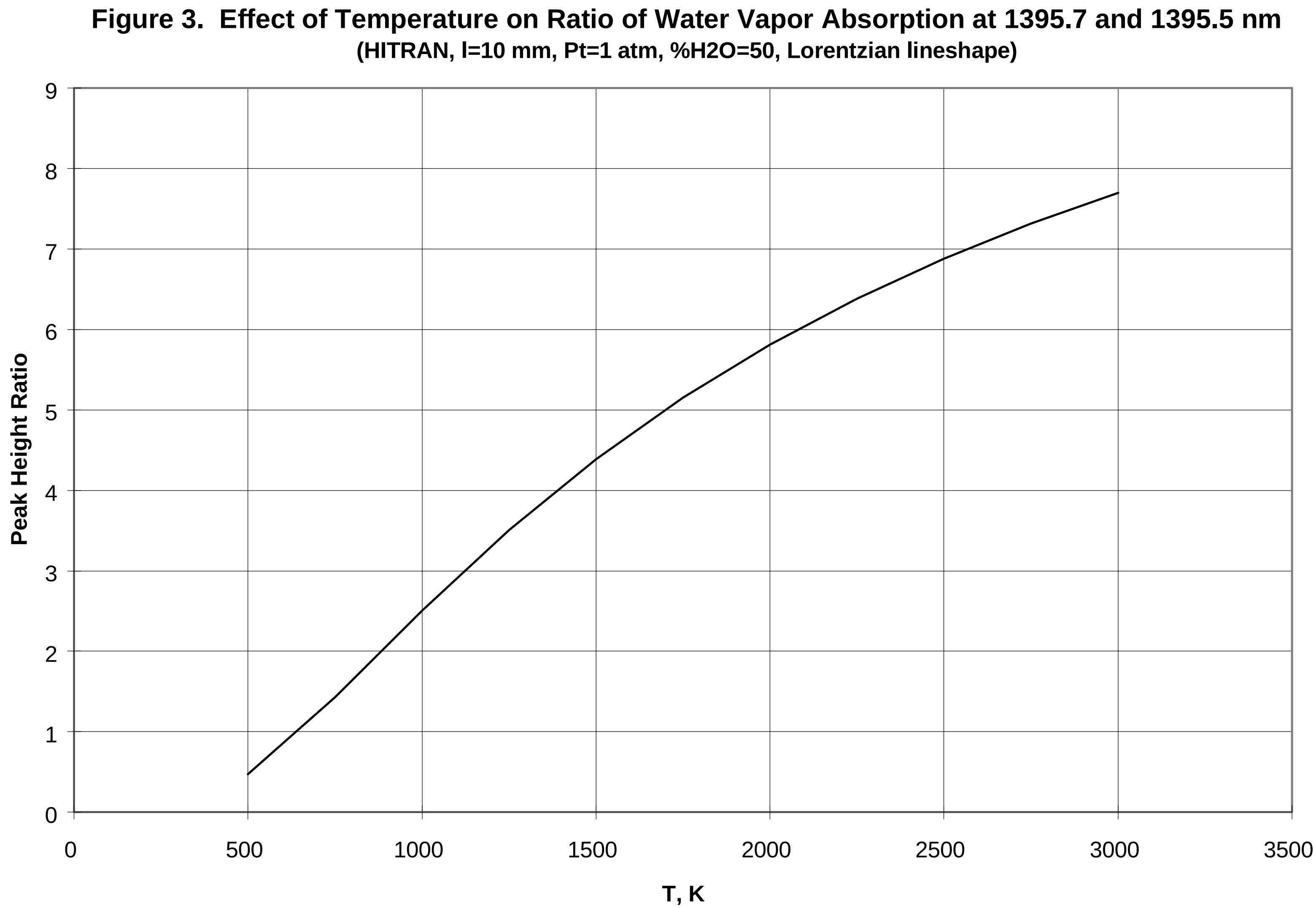
Figure 3. Effect of Temperature on Ratio of Water Vapor Absorption at 1395.7 and 1395.5 nm
(HITRAN, l=10 mm, Pt=1 atm, %H2O=50, Lorentzian lineshape)
Peak Height Ratio
0
1
2
3
4
5
6
7
8
9
0
500
1000
1500
2000
2500
3000
3500
T, K

Figure 4. The 3-beam Water Vapor Sensor System

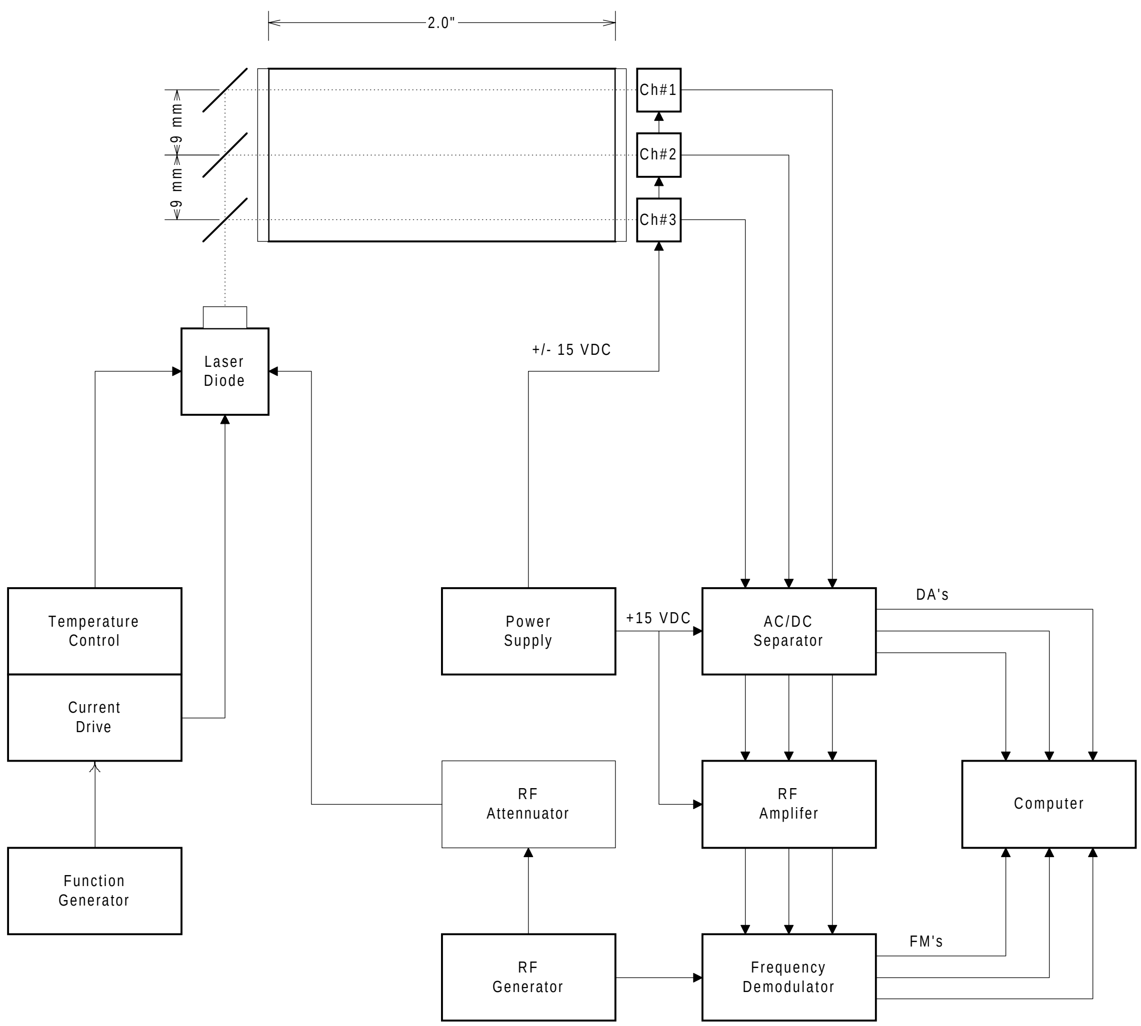

Figure 5. Water Vapor Sensor System Operated on the Flat Flame Burner

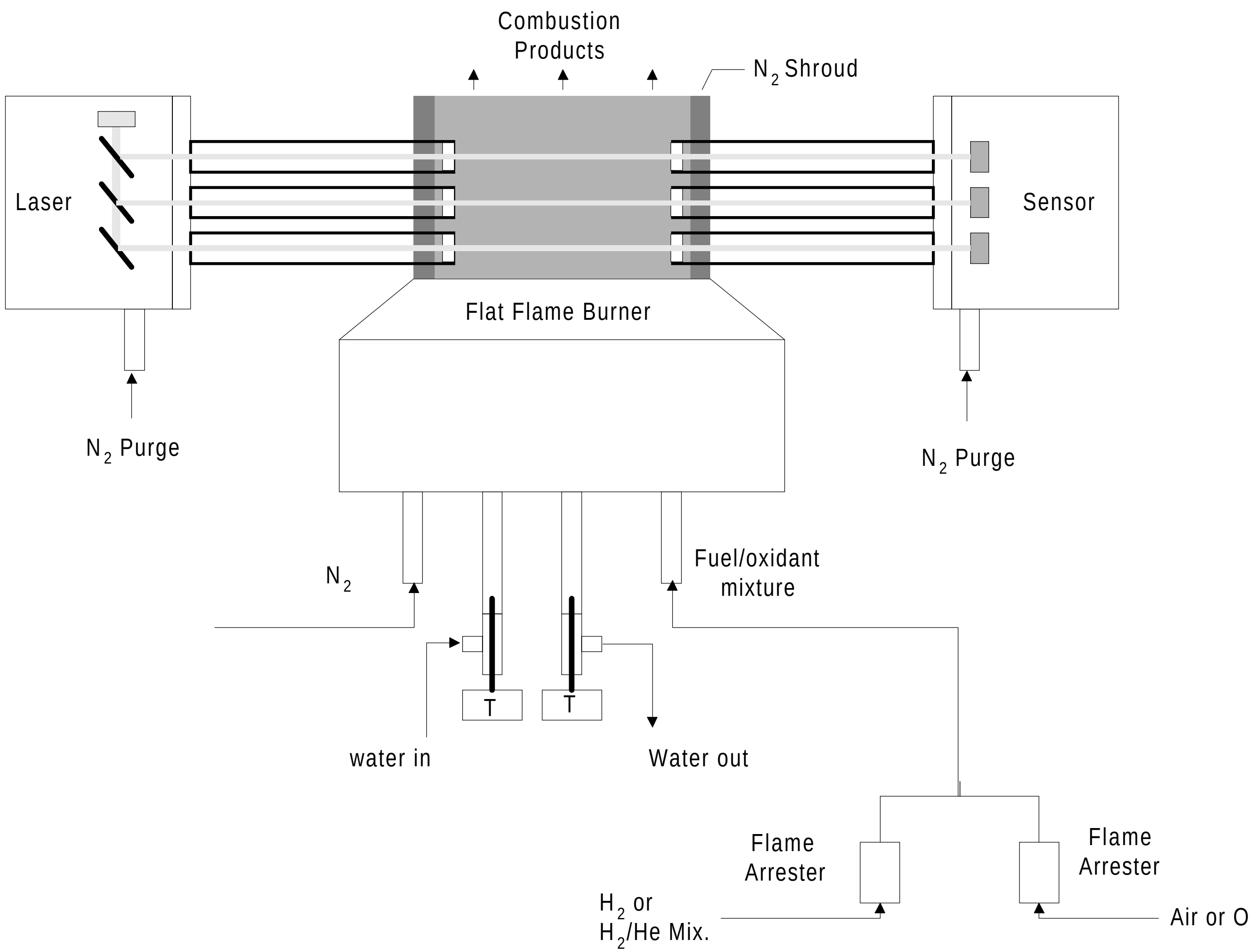

Figure 6. Estimated Temperature of Water Vapors Produced from the Flat Flame Burner

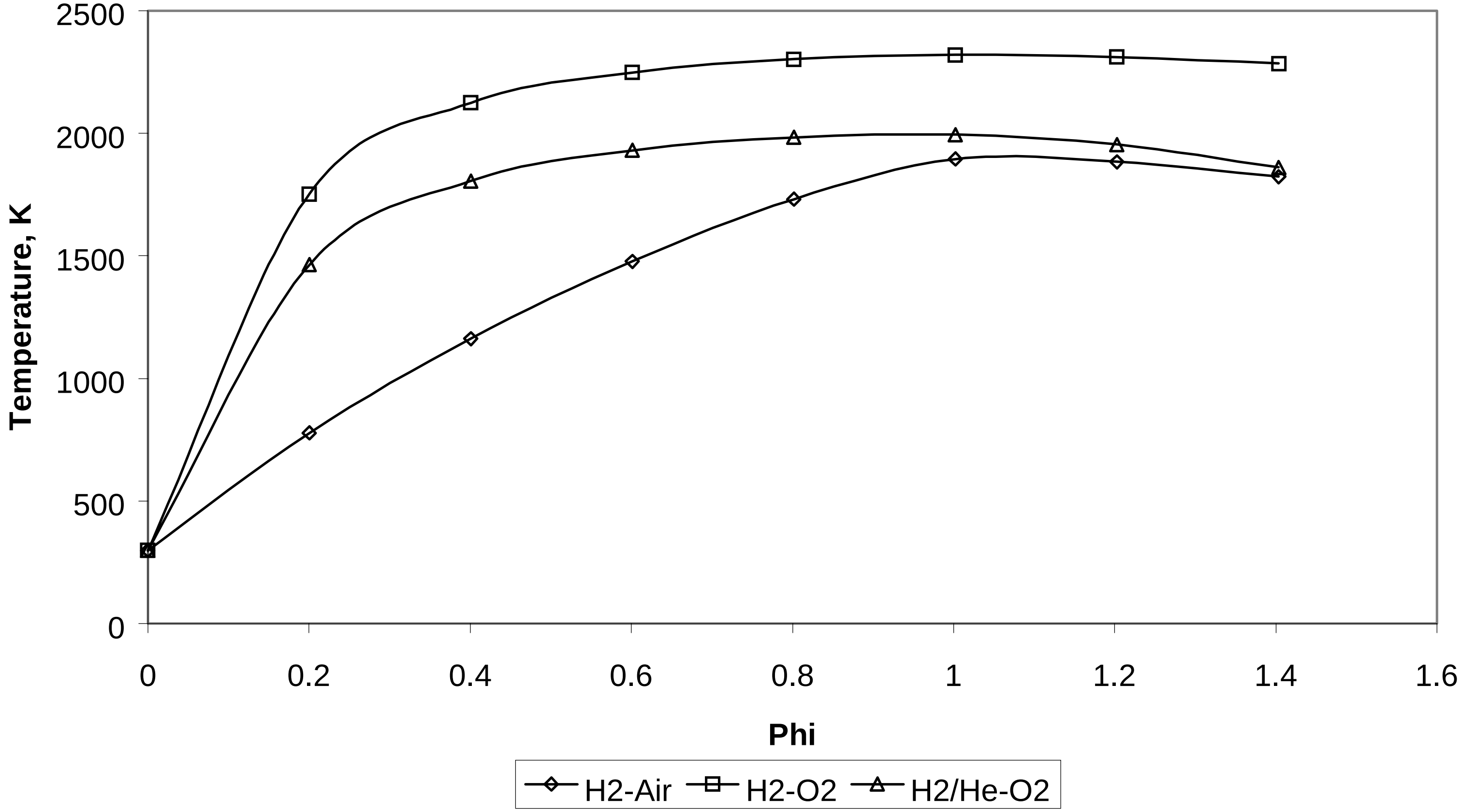

Figure 7. Concentration of Water Vapors Produced from the Flat Flame Burner

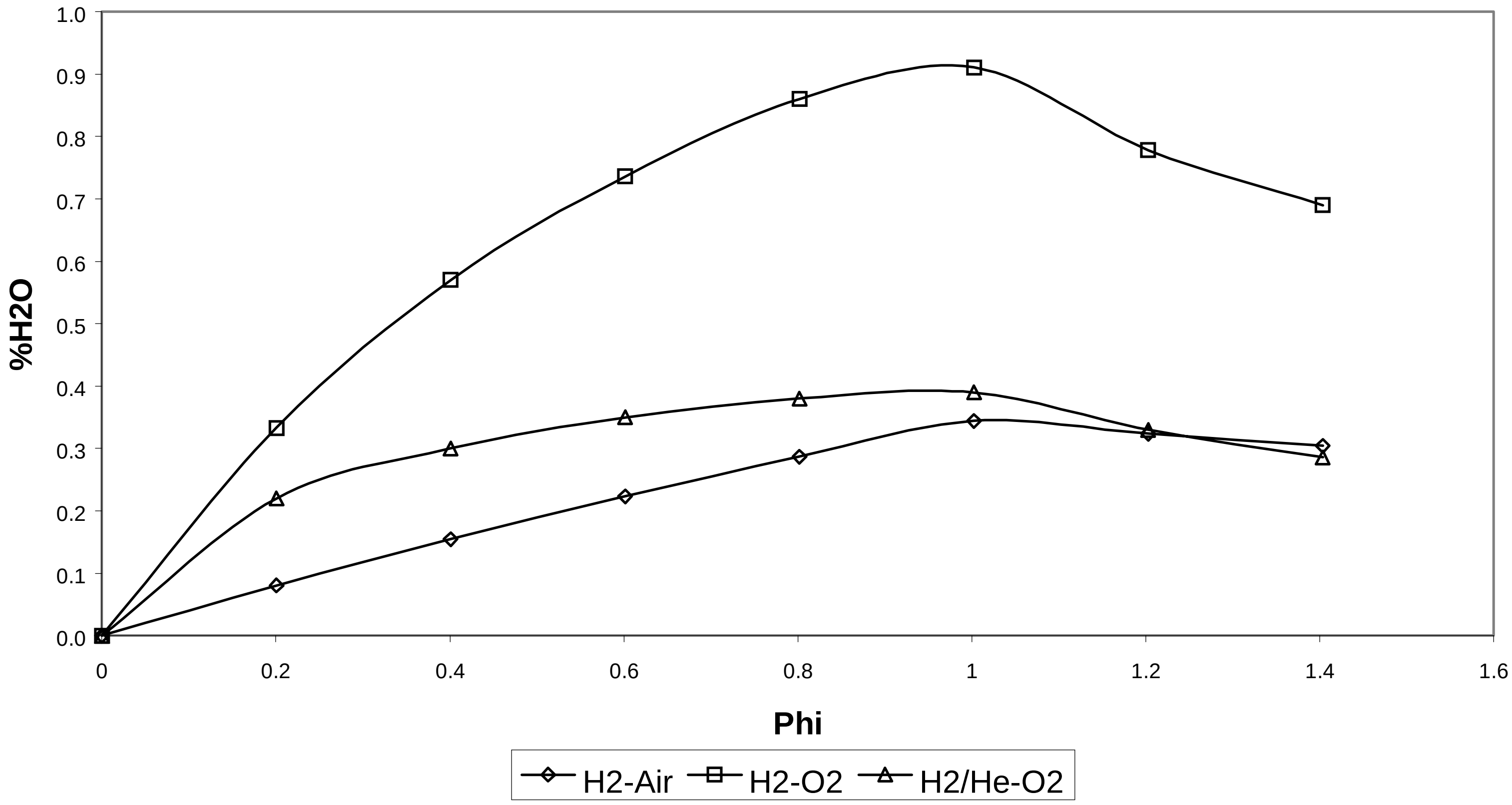

Figure 8. Test C04-ch#3 (H2-Air, phi=0.6)

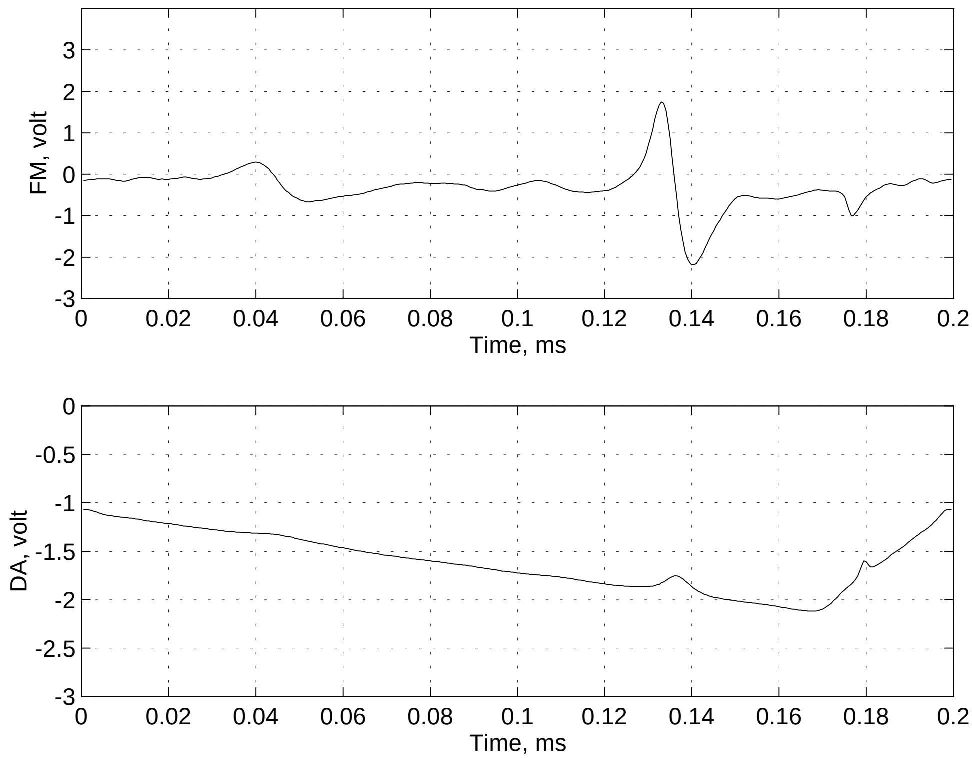

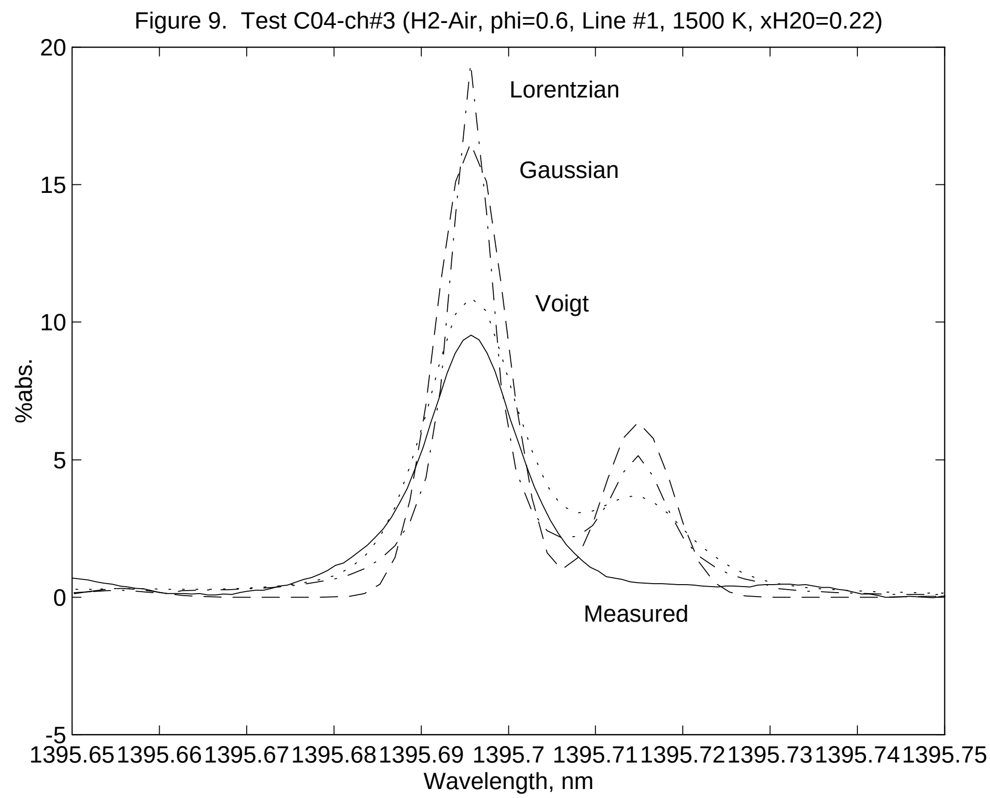
Figure 9. Test C04-ch#3 (H2-Air, phi=0.6, Line #1, 1500 K, xH20=0.22)
Lorentzian
Gaussian
Voigt
Measured
%abs.
20
15
10
5
0
-5
1395.65
1395.66
1395.67
1395.68
1395.69
1395.7
1395.71
1395.72
1395.73
1395.74
1395.75
Wavelength, nm

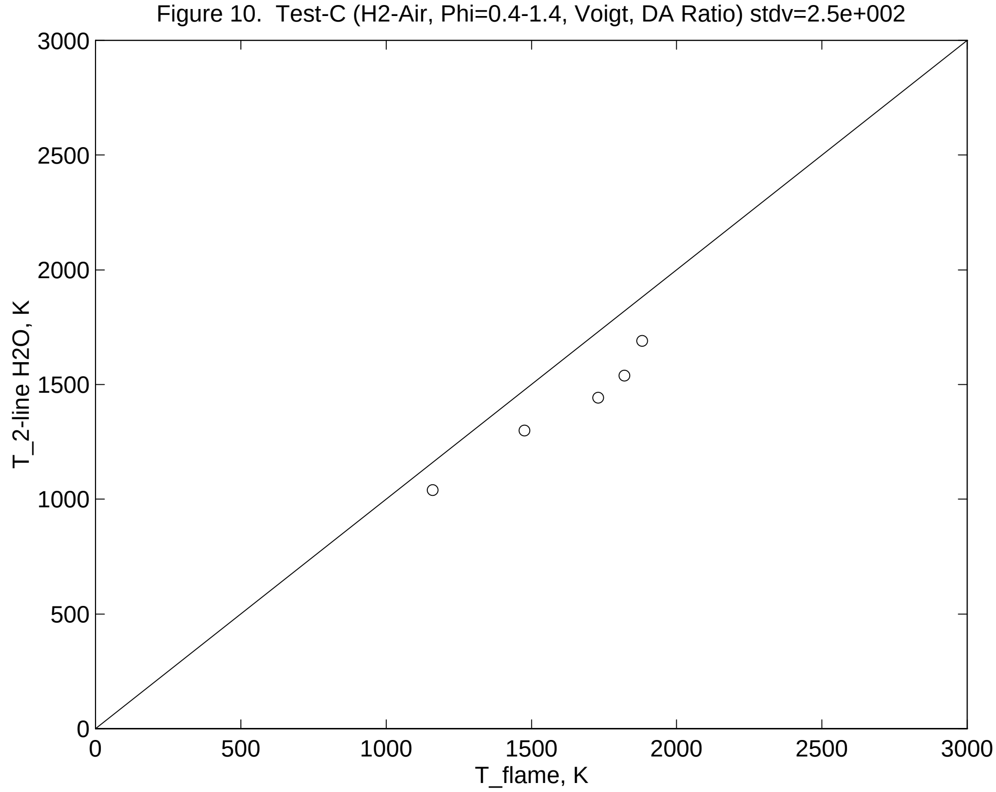

Figure 10. Test-C (H2-Air, Phi=0.4-1.4, Voigt, DA Ratio) stdv=2.5e+002
T_2-line H2O, K
T_flame, K
0
500
1000
1500
2000
2500
3000

Figure 11. Test-C (H2-Air, Phi=0.4-1.4, Voigt, Tc from DA Ratio) stdv=0.078

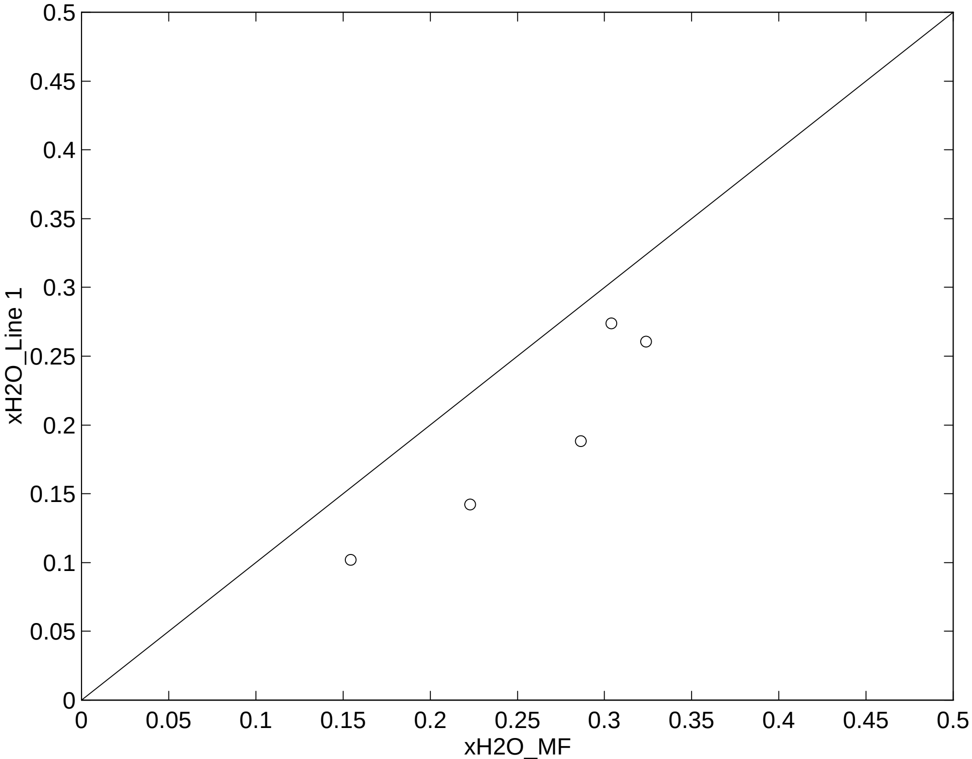

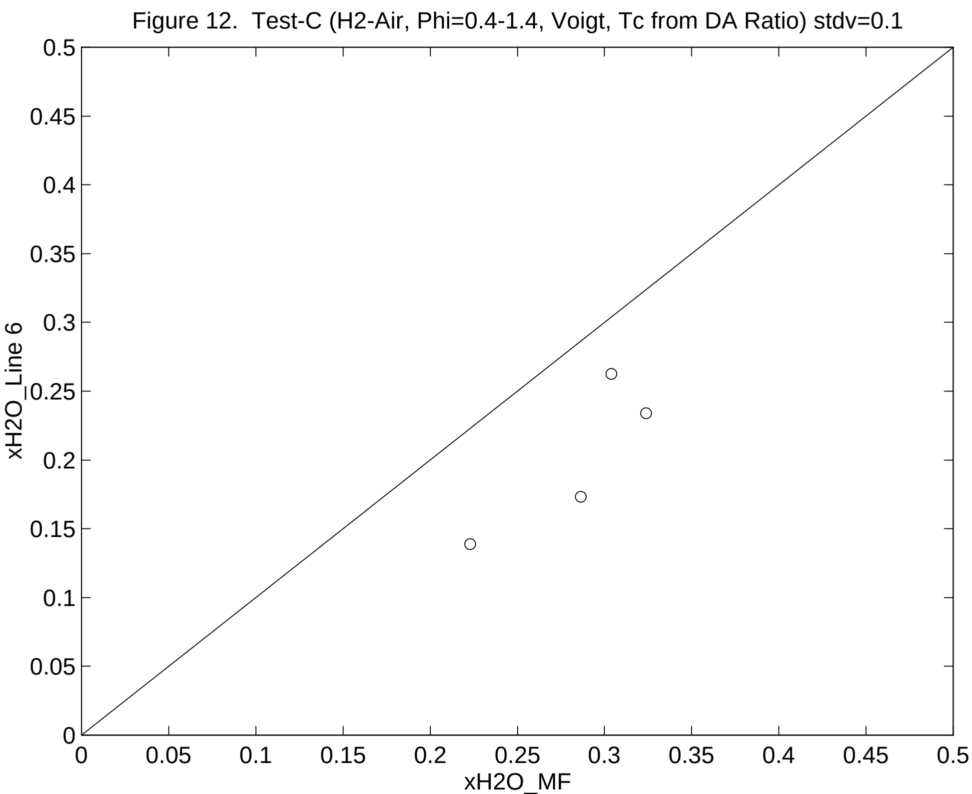
Figure 12. Test-C (H2-Air, Phi=0.4-1.4, Voigt, Tc from DA Ratio) stdv=0.1
xH2O_Line 6
xH2O_MF
0
0.05
0.1
0.15
0.2
0.25
0.3
0.35
0.4
0.45
0.5

Figure 13. Test G04-ch#3 (H2/He-O2, phi=0.6, 1930 K, xH20=0.35)

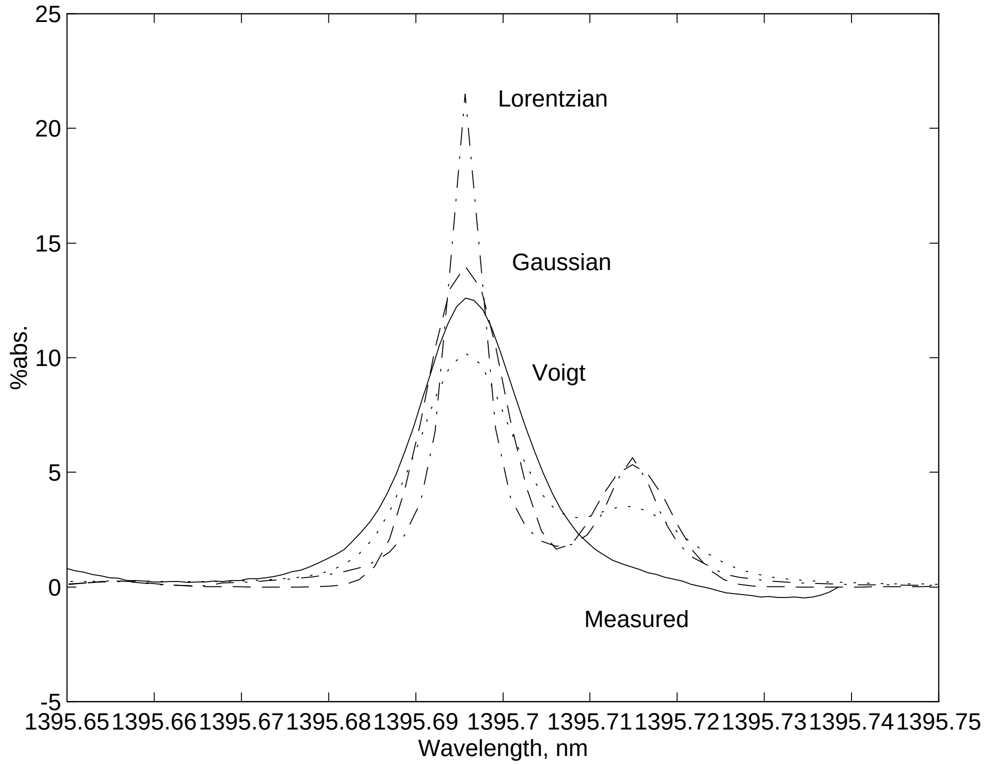

Figure 14. Test-G (H2/He-O2, Phi=0.2-1.2, Gaussian, DA Ratio) stdv=79

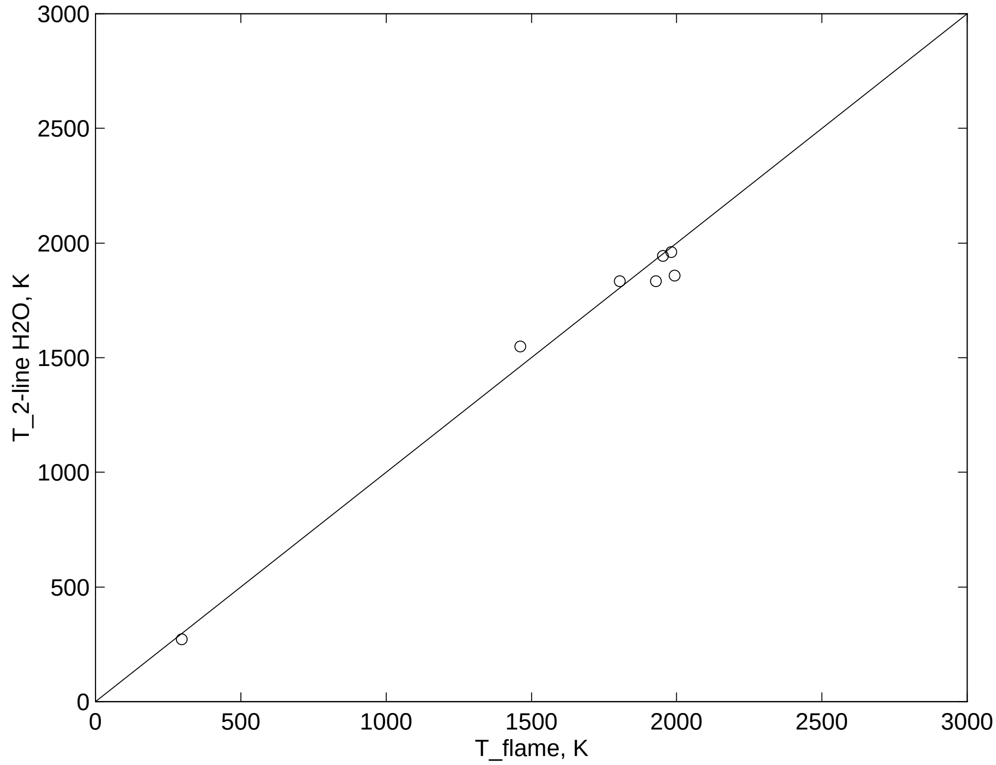

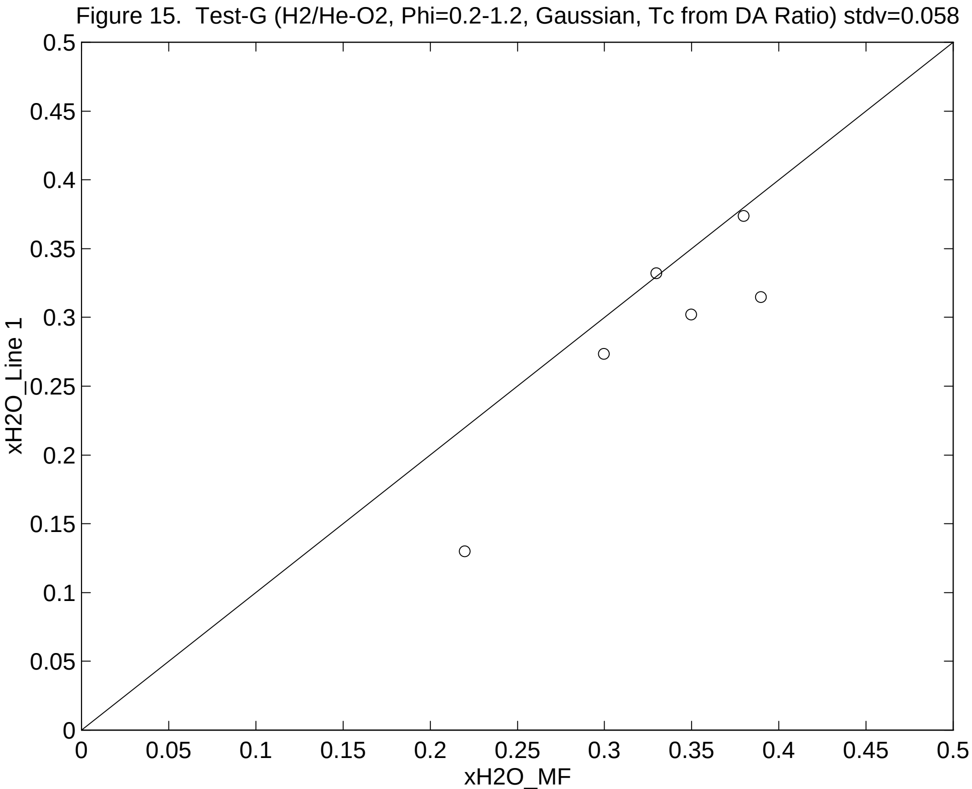
Figure 15. Test-G (H2/He-O2, Phi=0.2-1.2, Gaussian, Tc from DA Ratio) stdv=0.058
xH2O_Line 1
xH2O_MF
0
0.05
0.1
0.15
0.2
0.25
0.3
0.35
0.4
0.45
0.5

Figure 16. Test-G (H2/He-O2, Phi=0.2-1.2, Gaussian, Tc from DA Ratio) stdv=0.057

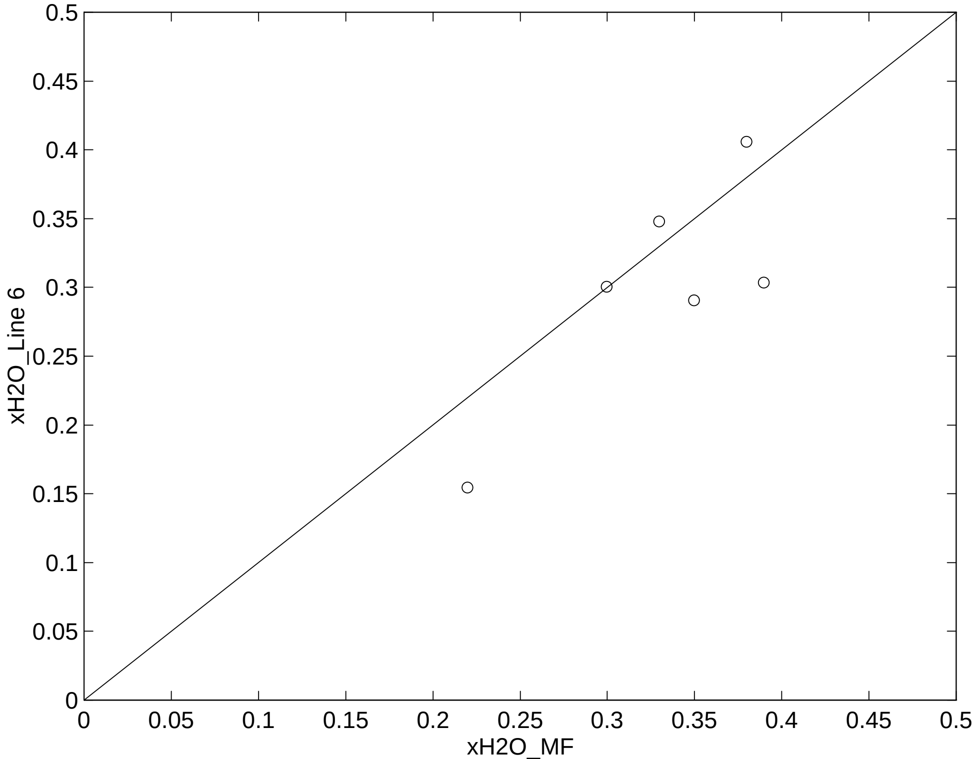

Figure 17. Test-D (H2-O2, Phi=0.2-1.2, Gaussian, DA Ratio) stdv=8.5e+002

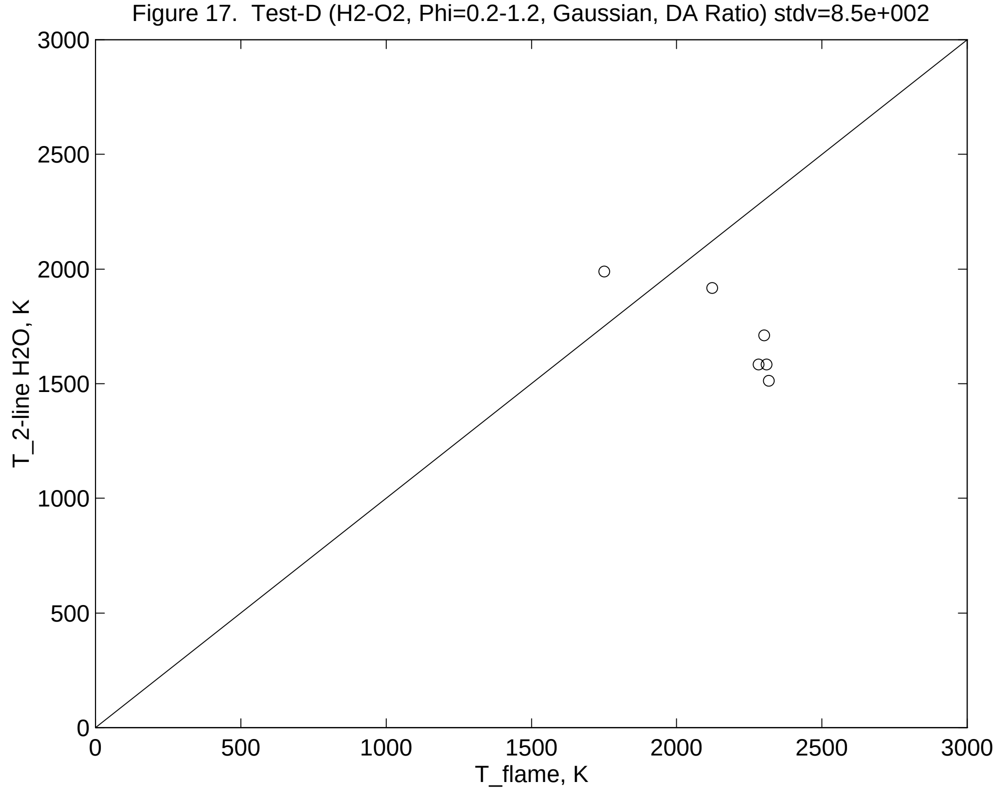

Figure 18. Test-F (H2-O2, Phi=0.2-1.2, Gaussian, DA Ratio) stdv=3.1e+002

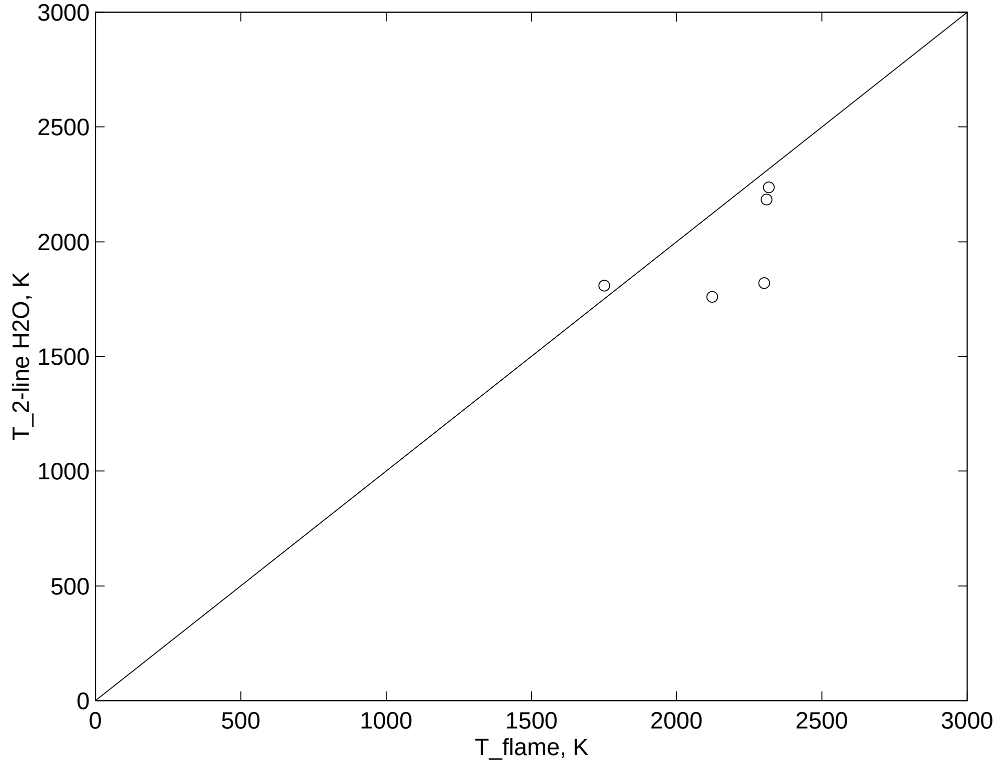

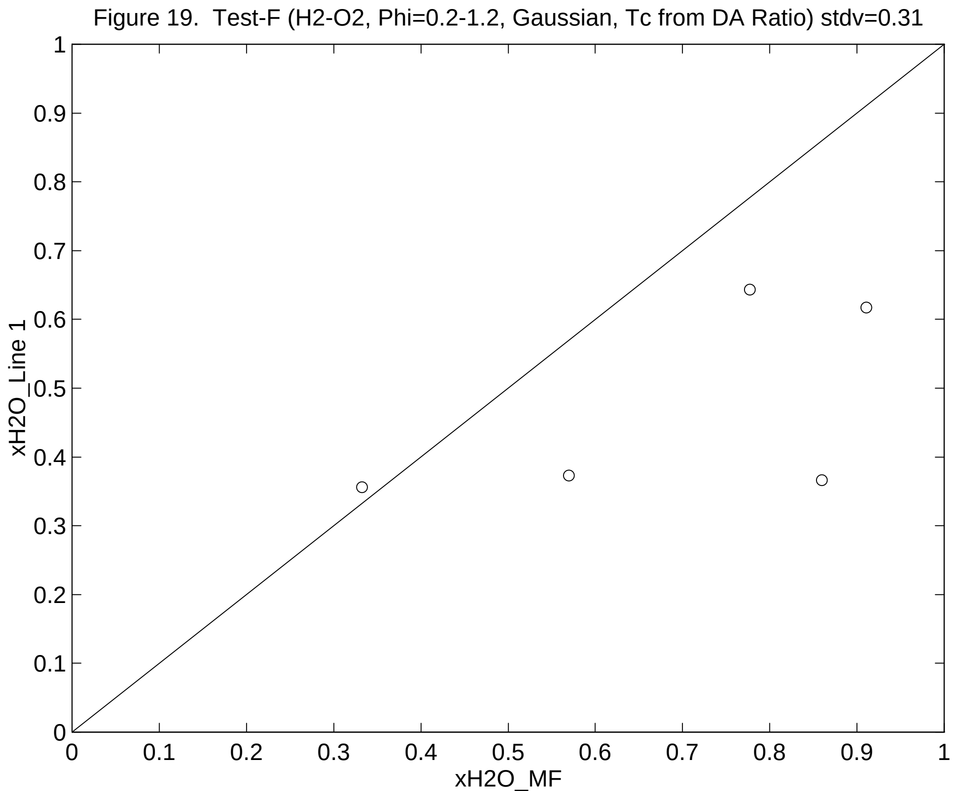
Figure 19. Test-F (H2-O2, Phi=0.2-1.2, Gaussian, Tc from DA Ratio) stdv=0.31
xH2O_Line 1
xH2O_MF
0
0.1
0.2
0.3
0.4
0.5
0.6
0.7
0.8
0.9
1

Figure 20. Test-F (H2-O2, Phi=0.2-1.2, Gaussian, Tc from DA Ratio) stdv=0.37

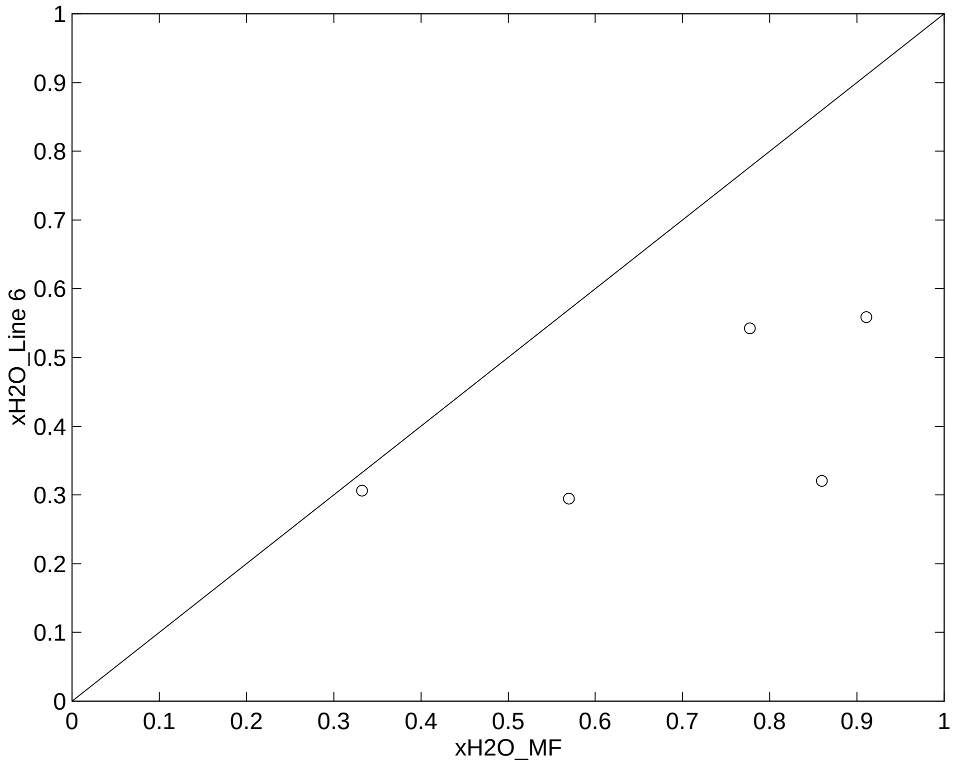

Figure 21. Test-C (H2-Air, Phi=0.4-1.4, Voigt, FM Ratio) stdv=42

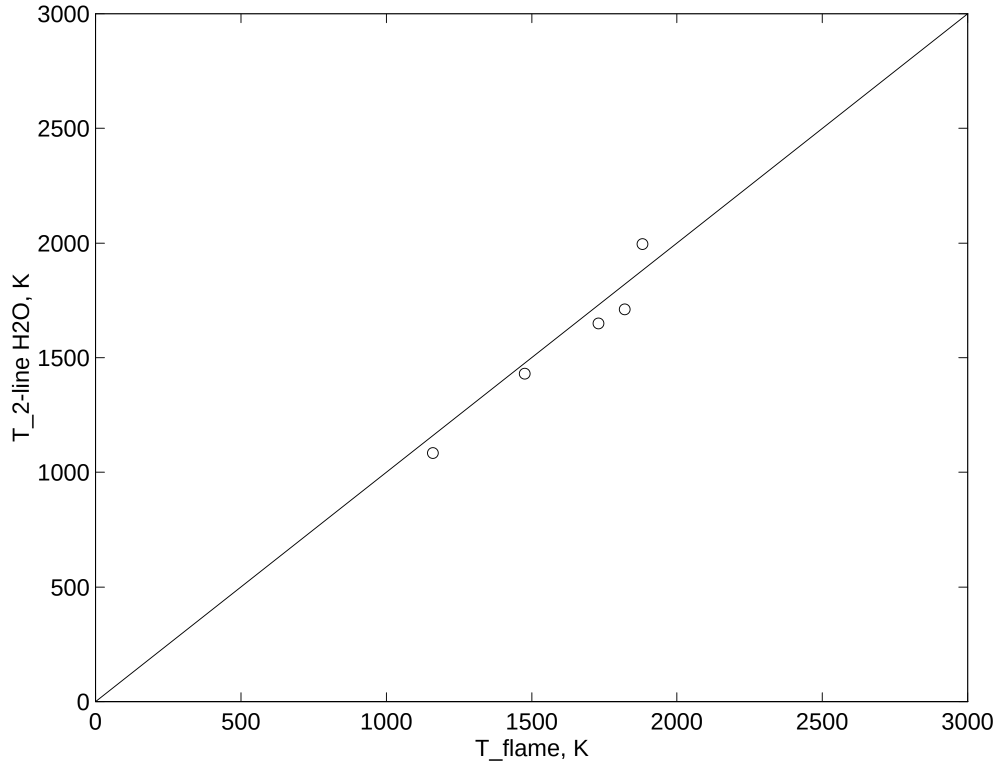

Figure 22. Test-G (H2/He-O2, Phi=0.2-1.2, Gaussian, FM Ratio) stdv=87

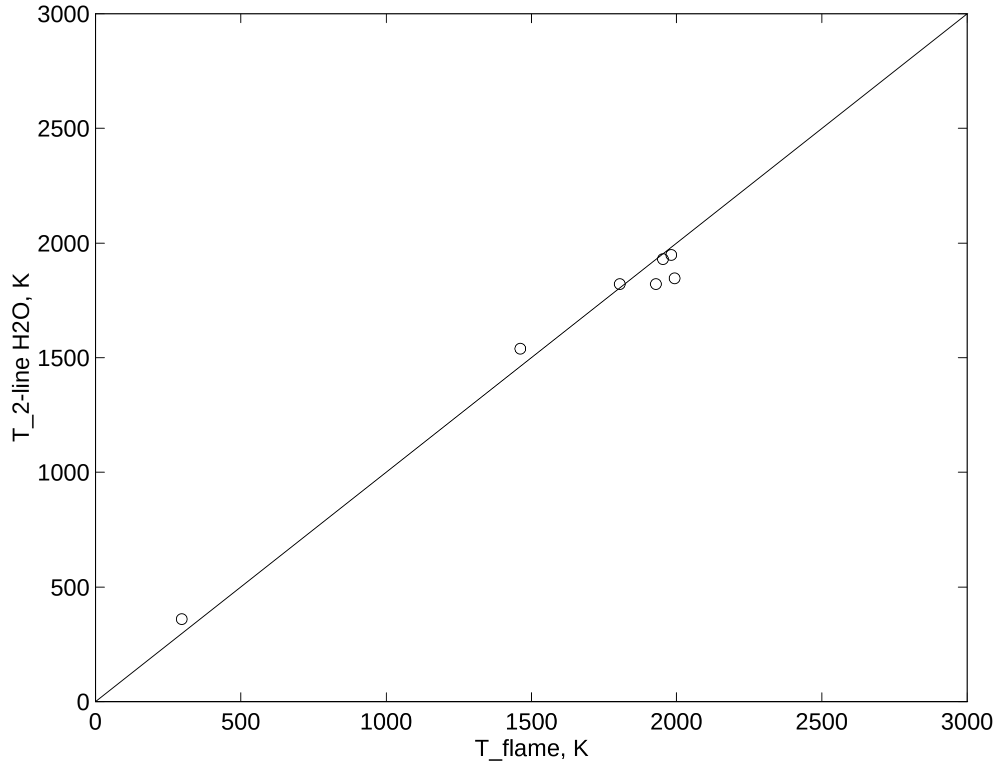

Figure 23. Test-F (H2-O2, Phi=0.2-1.2, Gaussian, FM Ratio) stdv=4.4e+002

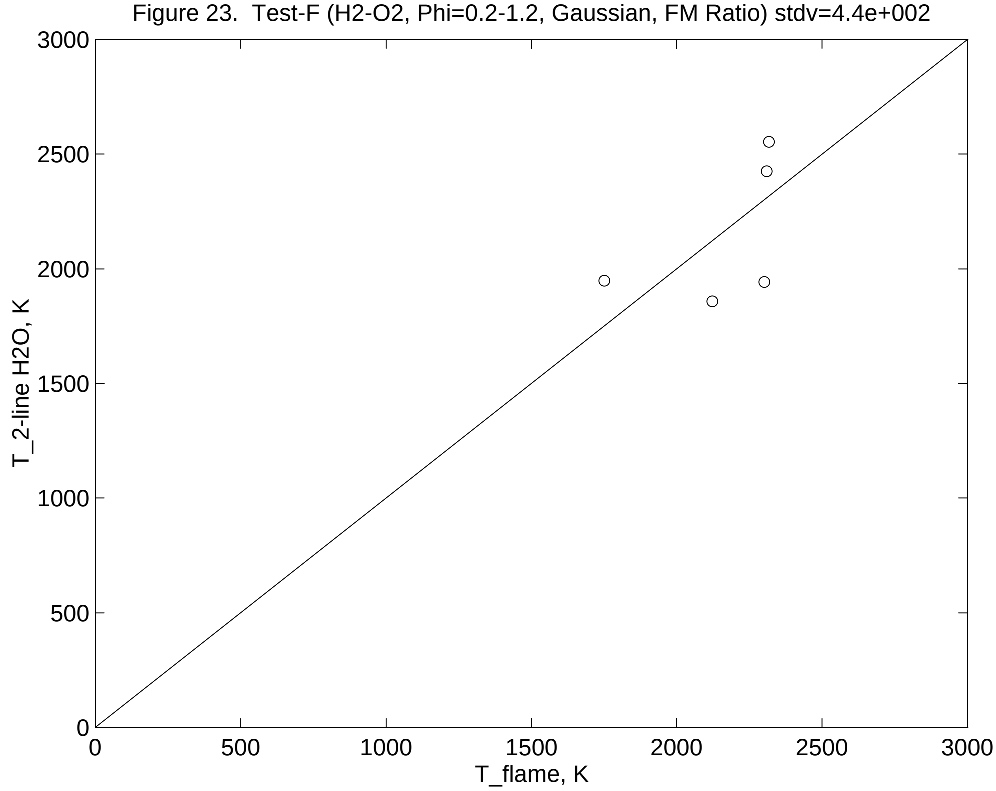

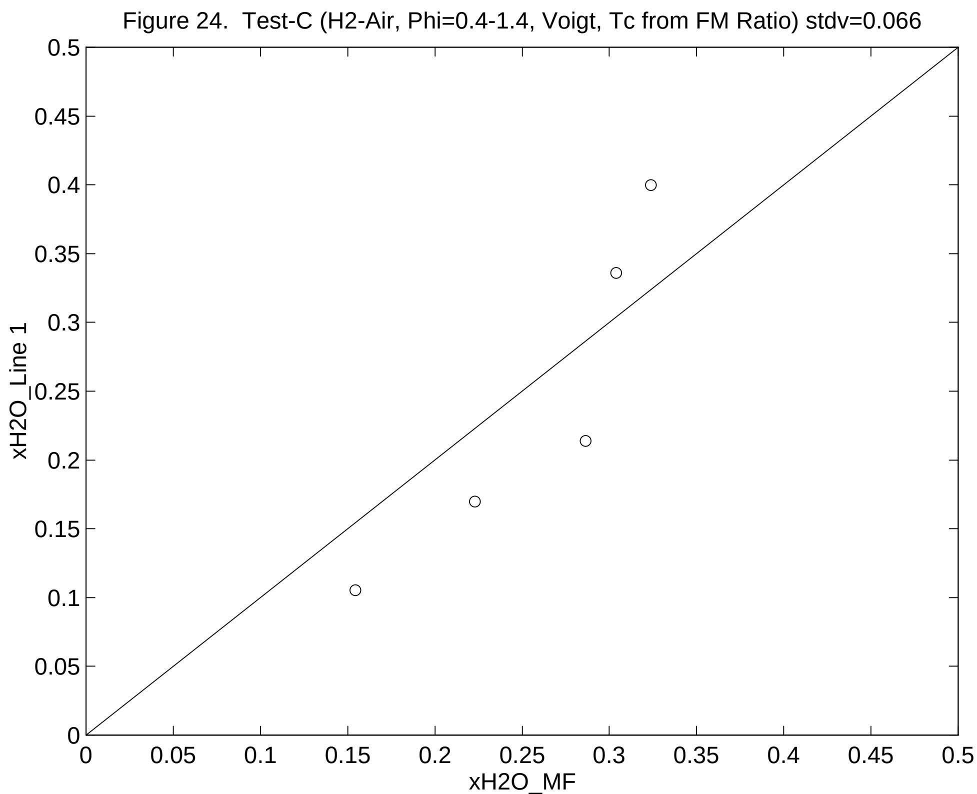
Figure 24. Test-C (H2-Air, Phi=0.4-1.4, Voigt, Tc from FM Ratio) stdv=0.066
xH2O_Line 1
xH2O_MF
0
0.05
0.1
0.15
0.2
0.25
0.3
0.35
0.4
0.45
0.5

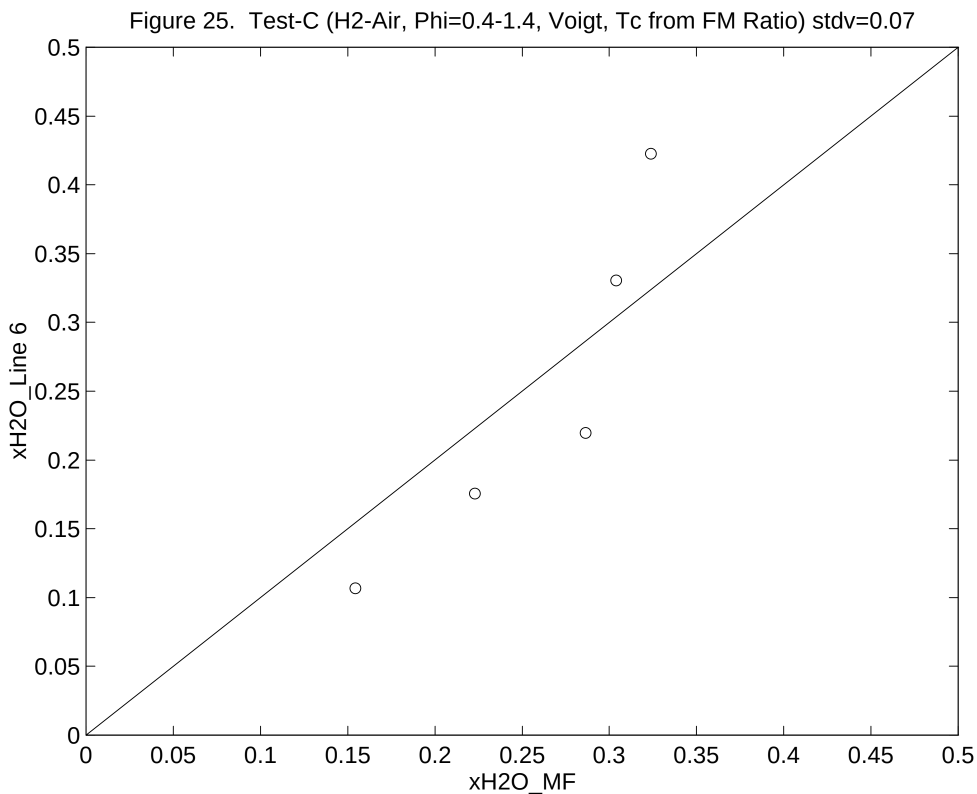
Figure 25. Test-C (H2-Air, Phi=0.4-1.4, Voigt, Tc from FM Ratio) stdv=0.07
xH2O_Line 6
xH2O_MF
0
0.05
0.1
0.15
0.2
0.25
0.3
0.35
0.4
0.45
0.5

Figure 26. Test-A (H2-Air w/ N2 Shroud, Phi=0.2-1.4, Voigt, DA Ratio) stdv=1e+003

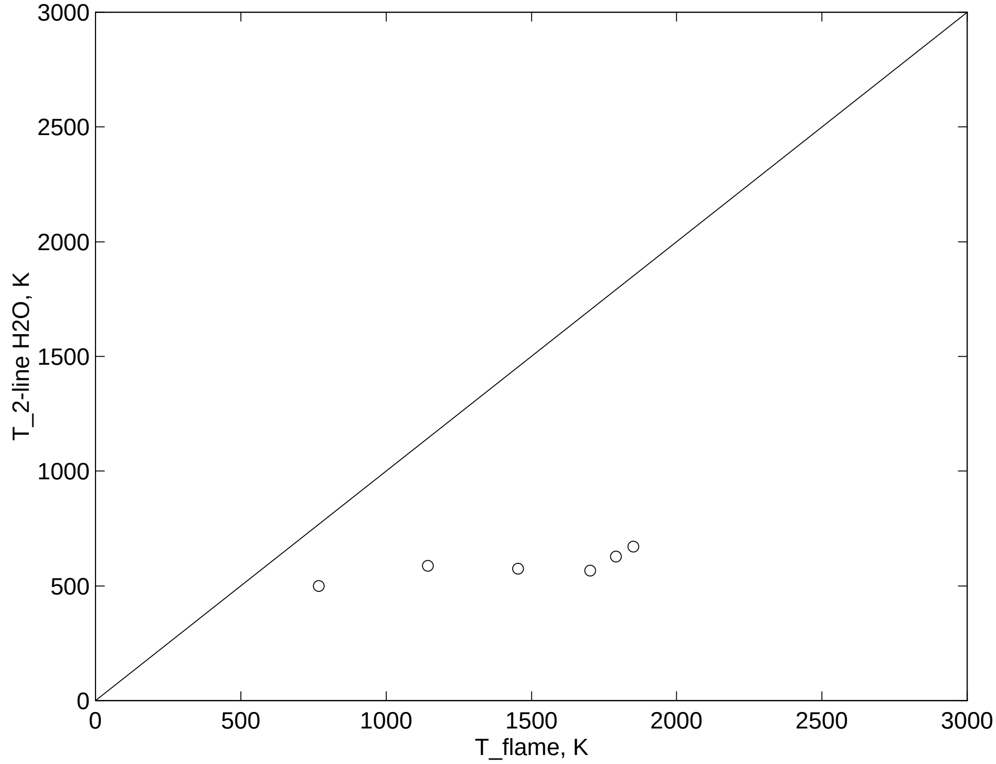

REPORT DOCUMENTATION PAGE			Form Approved OMB No. 0704-0188

Public reporting burden for this collection of information is estimated to average 1 hour per response, including the time for reviewing instructions, searching existing data sources, gathering and maintaining the data needed, and completing and reviewing the collection of information. Send comments regarding this burden estimate or any other aspect of this collection of information, including suggestions for reducing this burden, to Washington Headquarters Services, Directorate for Information Operations and Reports, 1215 Jefferson Davis Highway, Suite 1204, Arlington, VA 22202-4302, and to the Office of Management and Budget, Paperwork Reduction Project (0704-0188), Washington, DC 20503.

1. AGENCY USE ONLY (*Leave blank*)	2. REPORT DATE May 1998	3. REPORT TYPE AND DATES COVERED Contractor Report

4. TITLE AND SUBTITLE A Two-Line Absorption Instrument for Scramjet Temperature and Water Vapor Concentration Measurement in HYPULSE	5. FUNDING NUMBERS NAS1-19443, Task 24 505-70-62-01
6. AUTHOR(S) C. Y. Tsai	
7. PERFORMING ORGANIZATION NAME(S) AND ADDRESS(ES) GASL, Inc. 77 Raynor Ave. Ronkonkoma, NY 11779	8. PERFORMING ORGANIZATION REPORT NUMBER GASL TM-266
9. SPONSORING/MONITORING AGENCY NAME(S) AND ADDRESS(ES) National Aeronautics and Space Administration Langley Research Center Hampton, VA 23681-2199	10. SPONSORING/MONITORING AGENCY REPORT NUMBER NASA/CR-1998-207664

11. SUPPLEMENTARY NOTES
Langley Technical Monitor: R. Clayton Rogers

12a. DISTRIBUTION/AVAILABILITY STATEMENT	12b. DISTRIBUTION CODE
Unclassified-Unlimited Subject Category 35 Distribution: Nonstandard Availability: NASA CASI (301) 621-0390	

13. ABSTRACT *(Maximum 200 words)*
A three beam water vapor sensor system has been modified to provide for near simultaneous temperature measurement. The system employs a tunable diode laser to scan spectral line of water vapor. The application to measurements in a scramjet combustor environment of a shock tunnel facility is discussed. This report presents and discusses the initial calibration of the measurement system.

14. SUBJECT TERMS	15. NUMBER OF PAGES	16. PRICE CODE
diagnostics, scramjets, combustion	39	A03

17. SECURITY CLASSIFICATION OF REPORT	18. SECURITY CLASSIFICATION OF THIS PAGE	19. SECURITY CLASSIFICATION OF ABSTRACT	20. LIMITATION OF ABSTRACT
Unclassified	Unclassified	Unclassified	